International Civil Aviation Organization

NINETEENTH MEETING OF THE COMMUNICATIONS/NAVIGATION AND SURVEILLANCE SUG-GROUP (CNS SG/19) OF APANPIRG

Bangkok, Thailand, 21 – 25 July 2015

Agenda Item 5.2: Updates on national PBN implementation plan and PBN implementation issues

CATEGORY III GBAS (GAST-D) VALIDATION STATUS IN JAPAN

(Presented by Japan)

SUMMARY

This paper presents the summary of GAST-D (Category-III GBAS) SARPs validation activities of Japan. Japan has developed a GAST-D ground experimental prototype and a GAST-D airborne experimental system by following draft international standards. Flight trials were successfully conducted at New Ishigaki Airport with and without ionospheric disturbances.

1. INTRODUCTION

1.1 Electronic Navigation Research Institute (ENRI), Japan has been actively involved in the operational validation activities of GAST-D Baseline Development SARPs (BDS) by the ICAO Navigation Systems Panel (NSP). ENRI conducted a four-year program of operational validation of GAST-D BDS from April 2011 to March 2015 [1,2].

1.2 The program included developments of a prototype of GAST-D ground subsystem and a GAST-D airborne experimental system, and flight tests with the combination of the ground subsystem and the airborne experimental system. One of the major objectives of the program was to validate the GAST-D BDS in the magnetic low latitude region.

1.3 The purpose of this information paper is to share the results and experience of GAST-D development and validation activities by Japan under the low latitude ionospheric conditions which large part of the APAC region shares.

2. DISCUSSION

2.1 GAST-D ground subsystem

2.1.1 A prototype of GAST-D ground subsystem had been developed as a part of activities for GAST-D BDS validation. Purpose of the development included identification of additional requirements in lower levels under environment in Japan. ENRI had started development of the

prototype of GAST-D ground subsystem in contract with NEC Corporation from March 2012 and it had been delivered in September 2013.

2.1.2 It was designed in compliance with all requirements of the BDS, RTCA documents of Do-245A, Do-246D and Do-253C except for software integrity assurance and redundant hardware. However, fundamental processes to design and validate the prototype have been done according to the guidance of SAE (Society of Automotive Engineers, Inc.) ARP4754 and ARP4761. During the development phase, Total of 23 meetings for system safety design and validation were held with NEC Corp.

2.1.3 Dual frequency (L1/L2) GNSS receivers (Novatel Euro-3) are employed for reference receivers of the ground subsystem prototype for to make it easy to validate ionospheric threat mitigation, though the receiver is not certified as a GBAS ground reference receiver. The prototype can also broadcast GBAS messages for SBAS ranging sources. The following GAST-D integrity monitors are implemented to the prototype:

- Ionospheric spatial gradient monitor,
- Signal Deformation monitor,
- Code-Carrier-Divergence (CCD) monitor,
- Excessive acceleration monitor,
- Ephemeris monitor,
- RFI monitor.

Including IFM (Ionosphere Field Monitor), the prototype has all integrity monitors for CAT-I which are based on ENRI's another CAT-I prototype in Kansai International Airport. The prototype also has some novel functions for advanced researches, which are an option to use reference signal with CSAC (Chip Scale Atomic Clock) and implementation of an integrity monitor to detect multiple receiver faults [3]. During system design, it was recognized that area covered by an ephemeris monitor was not explicitly described in BSD.

The prototype of the GAST-D ground subsystem was installed at New Ishigaki airport (24.4ºN, 124.1ºE, 19.6ºN in magnetic latitude), Okinawa, Japan by February 2014. It has been operated continuously from March 2014. Ishigaki is located in the low magnetic latitude and is close to the Equatorial Ionization Anomaly crests (Figure 1).

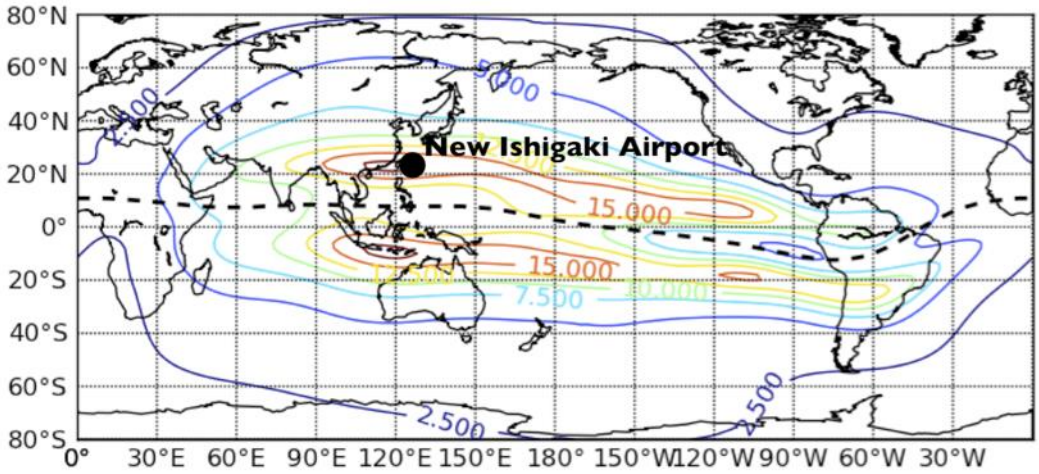

Figure 1. Location of the New Ishigaki Airport. Typical distribution of the ionospheric delay at the L1 frequency (1.57542 GHz) at 03 UT is also plotted.

2.1.4 The VDB transmitter antenna is a vertical stack of 3 folded-dipole antenna elements. The effective radiated power is 47 dBm.

2.1.5 The locations of components of the prototype are shown in Figure 2. The VDB transmitter antenna was installed on top of a ground-air communication antenna tower. Because the tower is located at a level about 15 m lower than the runway surface, the altitude of the VDB antenna is about 5 m above the runway surface. The location of the VDB transmitter antenna was chosen because it was the only location available for experimental GBAS system, although it might not have been ideal. The GAST-D ground prototype is supported by different ionospheric monitoring equipments near the airport including GNSS scintillation receiver network an all-sky airglow imager which can photograph the plasma bubble by detecting natural photon emission from the ionosphere (Figure 3).

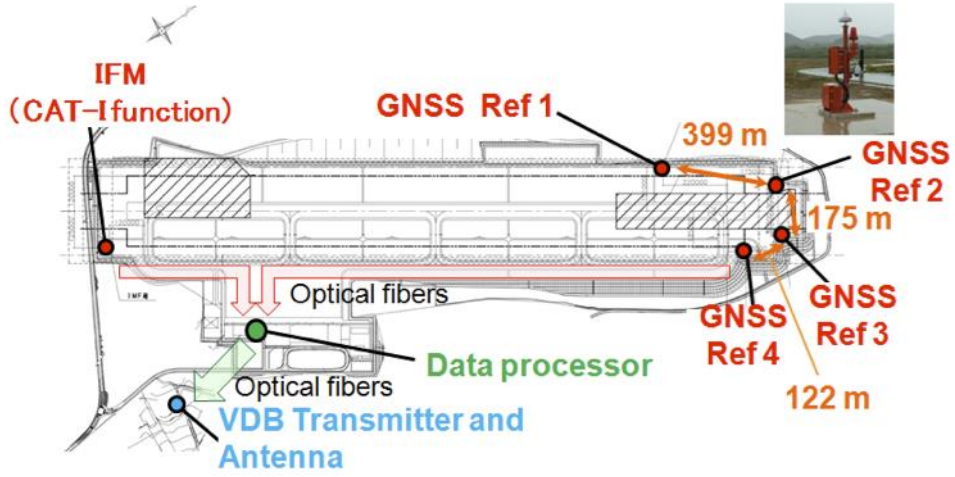

Figure 2. Locations of components of the prototype in the New Ishigaki airport.

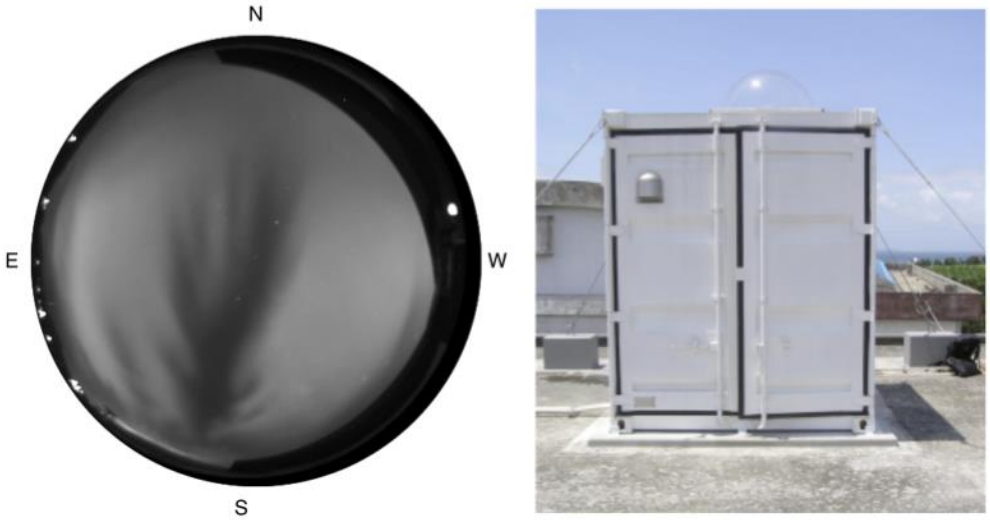

Figure 3. Left: Example of an all-sky image of plasma bubble at 630.0 nm wavelength (emission from atomic Oxygen). Right: The Ishigaki all-sky imager observatory.

2.1.6 Ionospheric Spatial Gradient monitor (ISGM) of the prototype is based on the single-frequency carrier-phase measurements aided by code measurements [4,5]. This monitoring algorithm

can estimate magnitude and direction of ionospheric spatial gradient with multiple baselines. It also enables us to validate estimated solution by consistency checks using a redundant baseline. Baseline length of 399 meters between GNSS reference station of RR1 and RR2 was enough separation judging from the former analysis of detectable sensitivity to observational error. Figure 4 shows actual estimated slant delay differences of ionospheric delay (δI_{SD}) between RR2 and RR1 under nominal condition. To detect the ionospheric gradient of 300 mm/km, ISGM for the pair of RR1 and RR2 must detect δI_{SD} of 119.7 mm (300mm/m x 0.399km). To achieve this with a fault-free detection (false alarm) probability less than $2 \cdot 10^{-7}$ and a missed-detection probability less than 10^{-9}, the threshold value of ISGM can be set from 51.3 to 60.5 mm. This means that the ISGM can be implemented so that it can detect 300mm/km gradient with satisfying the false alarm and miss-detection requirements.

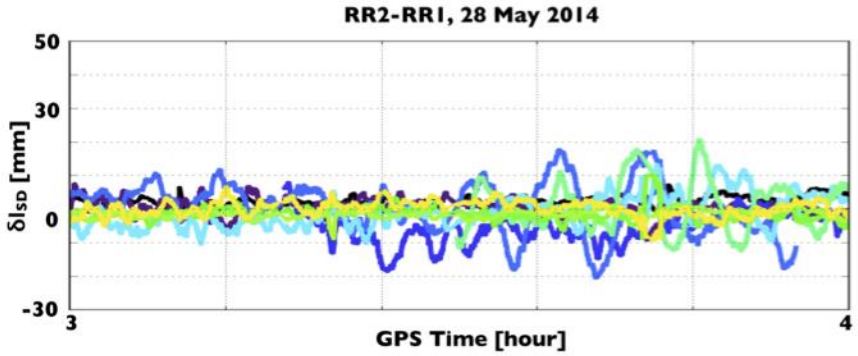

Figure 4. An example of estimated slant delay differences of ionospheric delay (δ ISD) between RR2 and RR1 with a baseline length of 399m from 03:00 to 04:00 on 28 May 2014. Different colors indicate different satellites [6].

2.1.7 Algorithm of Signal Deformation monitor (SDM) was evaluated using collected data at New Ishigaki Airport. Although there were some difficulties in validating the SDM in the designing phase of the monitor, where data collected on the roof of building were used, SDM algorithm of the prototype was feasible to meet with the requirements except measurements in low elevation angles from 5 to 10 degrees where multipath effects were significant. The result suggests that it would be necessary to employ antennas with better anti-multipath performance, such as multipath limiting antenna, for GAST-D reference stations instead of the current choke-ring antenna.

2.1.8 To evaluate the performance of GAST-D and GAST-C augmentation in long term, IFM station at approximately 2 km away from the GBAS reference point (GRP) is used as a pseudo-user. Table 1 shows position accuracy (95%) of the GAST-C and GAST-D solutions. The results are enough to meet with requirements and there are not significant differences between two seasons. It is also confirmed that positioning errors for GAST-D solutions are lager because of a shorter time smoothing constant. It should be noted that the conditions of the pseudo-user may be different from those of the real aircraft. For example, the distance from the pseudo-user and the GRP (2 km) is smaller than the possible distances between GRP and thresholds at large airports. The multipath condition may also be different on the ground and in the air. Thus, it is also important to evaluate the performance on board aircraft.

Table 1. Positioning accuracy (95%) of the prototype.

2014	GAST-C		GAST-D	
	Horizontal (m)	Vertical (m)	Horizontal (m)	Vertical (m)
March 21 - 27	0.1455	0.3848	0.2010	0.5212
August 07 - 13	0.1541	0.3705	0.2060	0.4938

2.2 GAST-D airborne subsystem

2.2.1 To close the loop of validation of the concept of integrity assurance of GAST-D BDS, a GAST-D airborne experimental system with which flight tests could be conducted was developed.

2.2.2 The experimental airborne system was developed with commercially available devices and the software was developed by ENRI based on the GAST-D BDS, RTCA DO-246D (LAAS ICD) and RTCA DO-253C (LAAS MOPS) with airborne monitors implemented. It can support both GAST-D and GAST-C (CAT-I) airborne processing.

2.2.3 Figure 5 shows the block diagram of the hardware of the airborne experimental system. The Javad Delta receiver was used for GAST-D navigation, while the Trimble NetR9 receiver was used to obtain true positions by Kinematic analysis by post-processing. The Telerad RE9009 receiver was used to receive VDB messages. It was supplied with a 1PPS signal to determine the slot of each message to support VDB authentication protocol. The Agilent N9010A Spectrum Analyzer was used to measure the VDB signal strength. All the data from the devices were corrected and processed by the PC, and the results were displayed on the cabin and cockpit displays in real time.

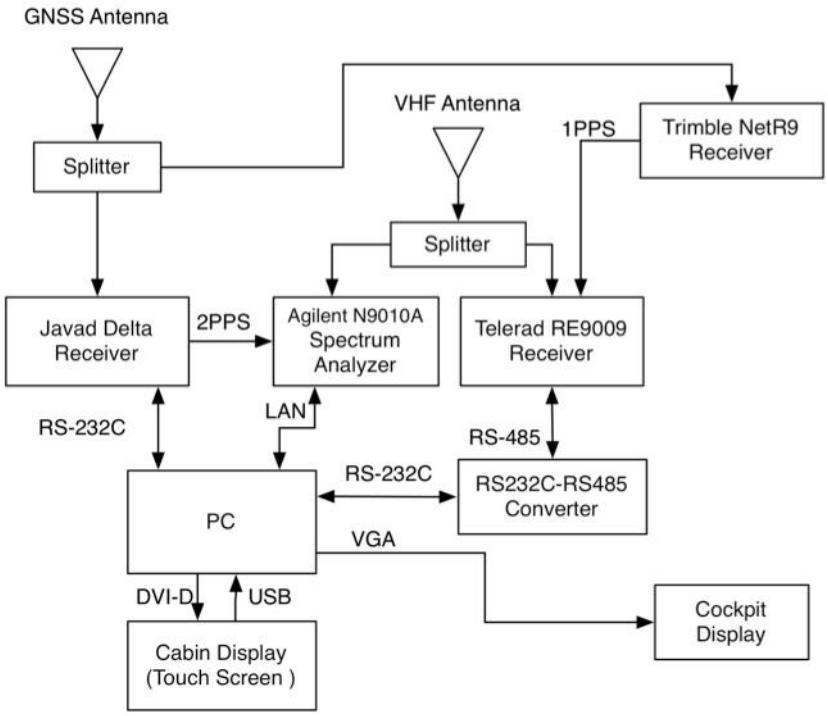

Figure 5. Block diagram of hardware.

2.2.4 The obtained and analyzed data were output to the cabin and cockpit displays as shown in the Figure 6.

2.2.5 The airborne experimental system was loaded on experimental racks in the cabin of the ENRI's experimental aircraft "Yotsuba" (Beechcraft King Air 350, Figure 7). The GNSS antenna for experiment was independent of that for aircraft operation and was equipped on the upper fuselage of the aircraft. The VHF antenna for experiment was also independent of that for aircraft operation and was equipped on the upper part of the vertical fin.

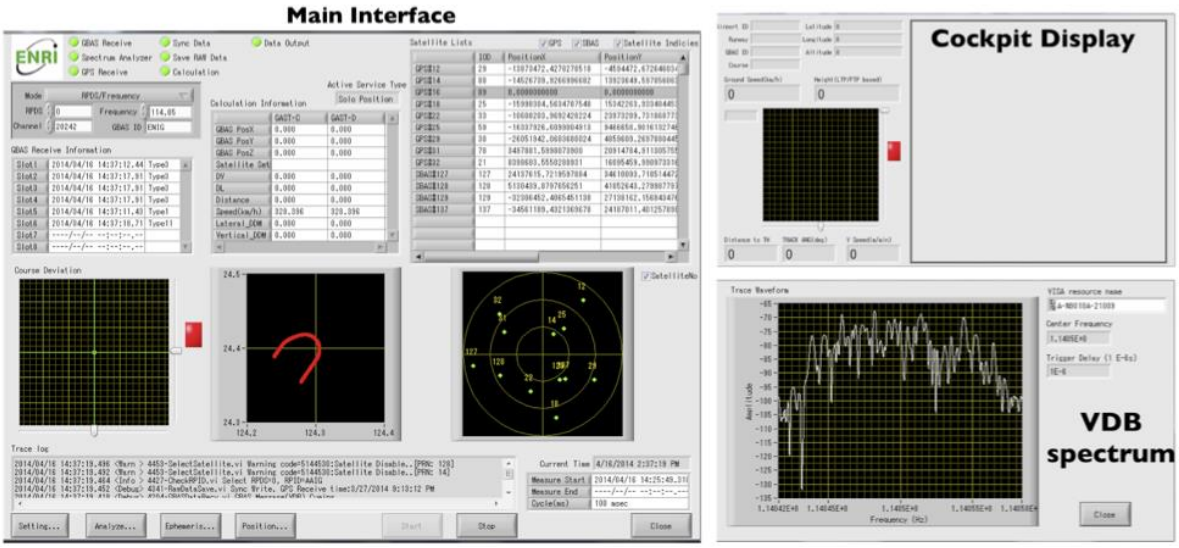

Figure 6. Interface of the GAST-D airborne experimental system.

Figure 7. ENRI's experimental aircraft "Yotsuba" (Beechcraft King Air 350).

2.3 GAST-D flight test

2.3.1 Two flight test campaigns were conducted from 21 to 28 March and from 15 to 23 September 2014. The periods were in the season when the plasma bubble, which is the major ionospheric disturbance in the low latitude region, occurs frequently. Those periods were also around the new moon period when the optical measurement of plasma bubbles by the all-sky imager was possible. The objectives of the flight test were

- Performance evaluation of the approach service
- VDB coverage check

To accomplish these objectives, seven flight patterns were designed as shown in Figure 8.

2.3.2 In the first flight campaign from 21 to 28 March 2014, 10 flights (6 in the day and 4 in the night) were flown. The flight schedule and flight patterns were summarized in Table 2. In total, 45 approaches (24 for RWY-22 and 21 for RWY-04) were conducted. Among the four nights of flight experiment, plasma bubbles occurrences were inferred by scintillation measurements in three nights. Although the sky was often partially cloudy, plasma bubble images were taken during the approaches of flight experiment on 28 March 2014.

Pattern 1 (Orbit-1) Radius: 20 nm, Altitude 5,000-10,000 ft	Pattern 2 (Orbit-2) Radius: 15 nm, Altitude 1,500 ft
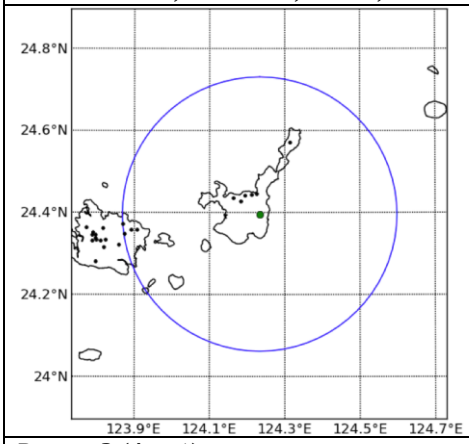	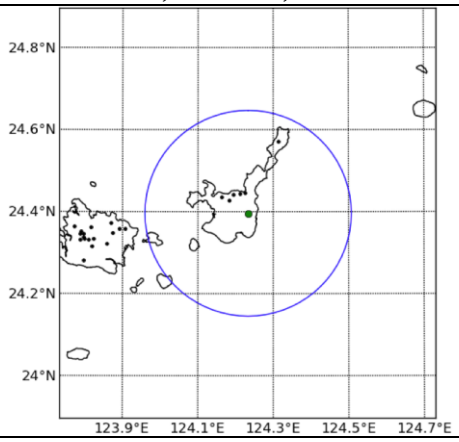
Pattern 3 (Arc-1) Radius: 20 nm, Altitude: 2,000 ft Azimuth: -45 to 225º (Magnetic)	Pattern 4 (Level-1) Length: 50 nm (25 nm both sides), Altitude: 10,000 ft
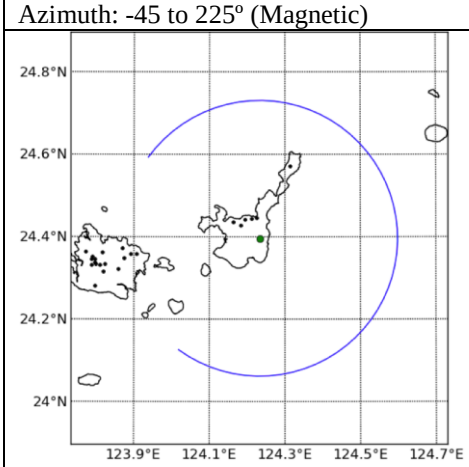	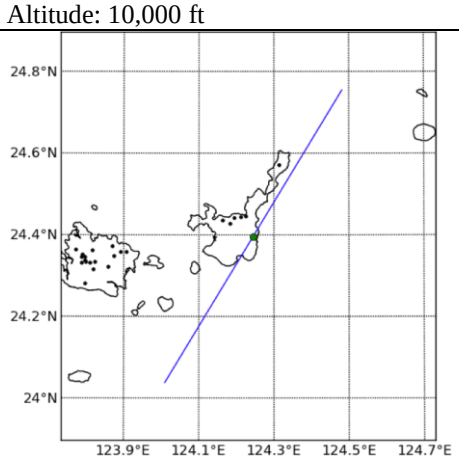
Pattern 5 (Level-2) Length: 50 nm (25 nm both sides), Altitude: 2000 ft	Pattern 6 (Approach-1) Length: 20 nm, RWY-04, GP: 3º
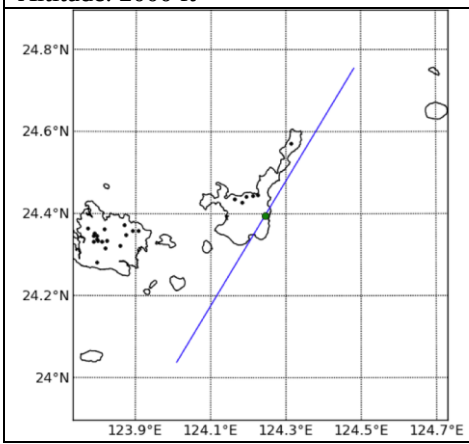	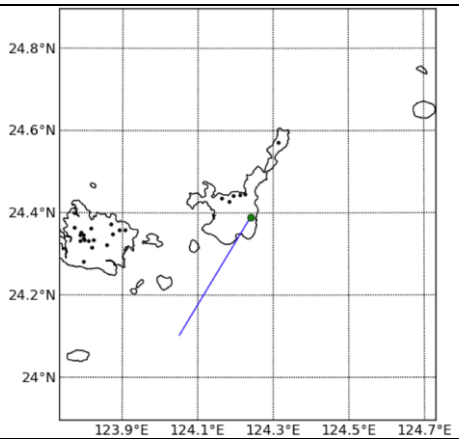

Figure 8. Flight patterns. Black dots on the map represents major mountains higher than 1,000ft.

Pattern 7 (Approach-2) Length: 20 nm, RWY-22, GP: 3º	
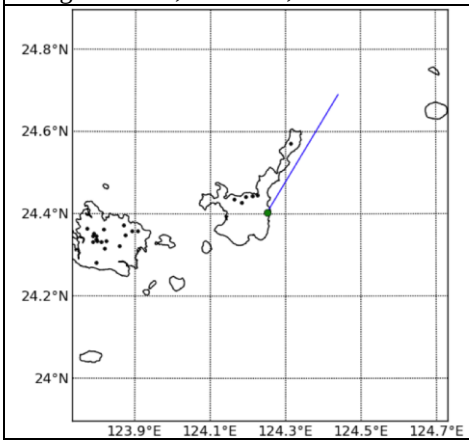	

Figure 8 (Cont'd). Flight patterns. Black dots on the map represents major mountains higher than 1,000ft.

Table 2. Flight schedules in the first flight campaign in March 2014.

Date	21 Mar. 2014	22 Mar. 2014	23 Mar. 2014	24 Mar. 2014
Day	Pattern 6	Pattern 2	Pattern 1	-
Night	Pattern 7	Pattern 6 *Plasma bubble	Pattern 5 plus 2 more approaces *Plasma bubble	-
Date	25 Mar. 2014	26 Mar. 2014	27 Mar. 2014	28 Mar. 2014
Day	Pattern 3	Pattern 7	-	Pattern 4&2
Night	-	-	-	Pattern 6&7 *Plasma bubble with all-sky-imager

Table 3. Flight schedules in the first flight campaign in March 2014.

Date	15 Sep. 2014	16 Sep. 2014	17 Sep. 20144	19 Sep. 2014	23 Sep. 2014
Day	Pattern 7	Pattern 1&7	Pattern 2&7	-	-
Night	Pattern 6&7 *Plasma bubble	Pattern 6	-	Pattern 6&7	Pattern 6&7 *Plasma bubble

2.3.3 In the second flight campaign from 15 to 23 September 2015, 7 flights (3 in the day and 4 in the night) were flown. The flight schedule and flight patterns were summarized in Table 3. In total, 32 approaches (18 for RWY-22 and 14 for RWY-04) were conducted. Among the four nights of flight experiment, plasma bubbles occurrences were inferred by scintillation measurements in two nights.

2.3.4 Figure 9 shows the results of the flight tests in the night of 23 September 2014. As seen in the bottom panel, there were 7 approaches (4 for RWY-22 and 3 for RWY-04). During the event, plasma bubbles were observed by the all-sky imager. The top panel shows the vertical error (green), vertical protection level (VPL, blue) and vertical alert limit (VAL, red). The vertical error was defined as the difference of vertical position obtained by GAST-D from the kinematic GNSS

solution. Since VAL is more than 40 m at longer distances from the threshold, only VAL less than 25 m can be seen. During the flight, there were no event when the vertical error exceeded the VPL. The 95% vertical error was 0.86 m, and the mean vertical error was 0.084 m.

2.3.5 During the course of the flight, there were a few periods of the output of DSIGMA for vertical position component (DV) as shown in the mid panel of Figure 9. For example, there were DV enhancements from 12:15 to 12:23, from 12:26 to 12:30, and from 13:37 to 13:40 GPS Time. The enhancements were up to 0.7 which was still below the DSIGMA monitor threshold (2 m) but significantly higher than the mean value (0.051 m) through this flight. During the period from 12:15 to 12:23 and from 12:26 to 12:30, the satellite PRN02 was found to be affected by the plasma bubble according to the all-sky airglow image (Figure 10a). In this figure, airglow in the direction of satellite PRN02 was masked by clouds. However, previous images indicates that there was a blanch of the plasma bubble in the right direction. From 13:37 to 13:40, the satellite PRN05 was also found to be affected by the plasma bubble (Figure 10b). Thus, it was confirmed that the DSIGMA monitor responded to ionospheric gradients, as it was expected.

2.3.6 As a summary, ENRI conducted two GAST-D flight trial campaigns with the GAST-D ground prototype and the GAST-D airborne experimental system both developed by ENRI. Flight tests were conducted in different conditions including day/night, and ionospheric disturbed/quiet conditions. The results from one of the disturbed nights showed that the GAST-D worked well to bound aircraft error to be as small as 0.86 m. The output of the airborne DSIGMA monitor was shown to be enhanced when a satellite was affected by a plasma bubble. And it was confirmed that the DSIGMA monitor worked as it was expected.

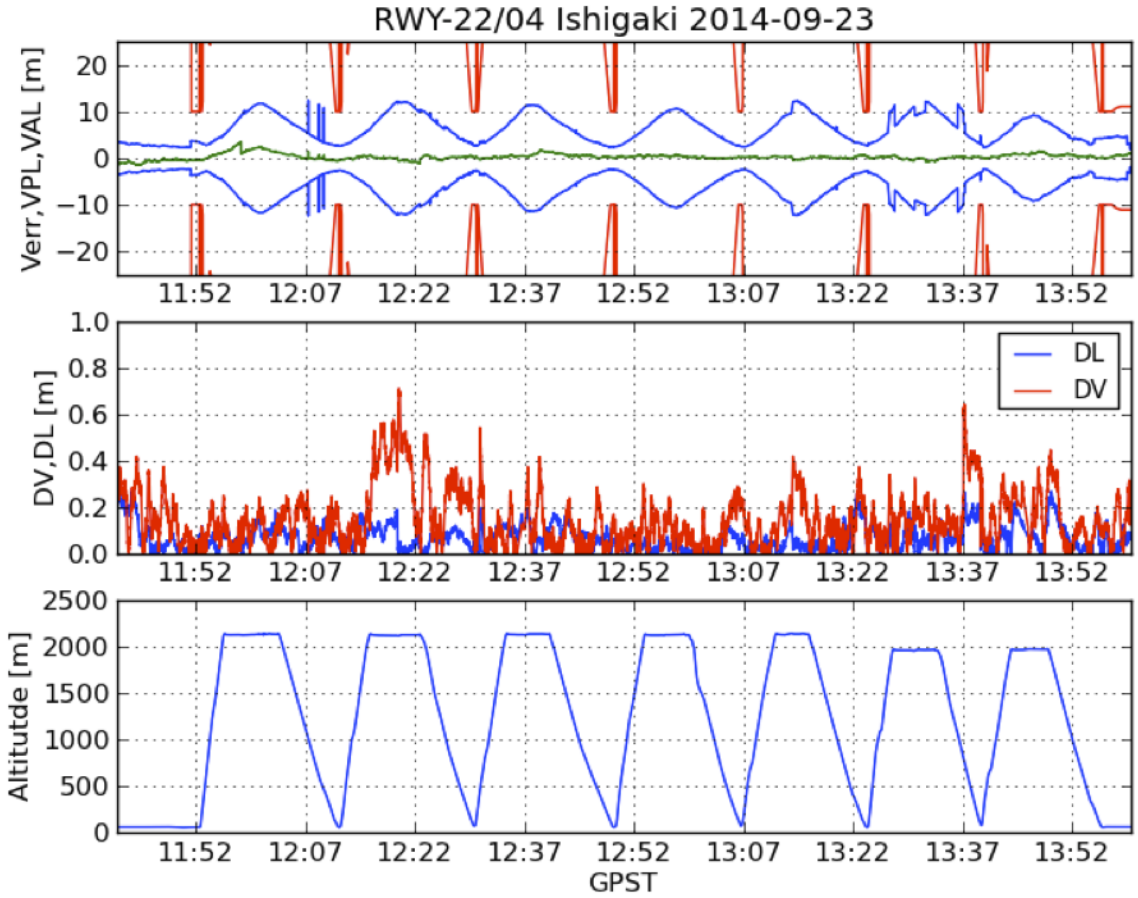

Figure 9. Flight test results on 23 September 2014. GPST is 9 hours behind the Japan Standard Time.

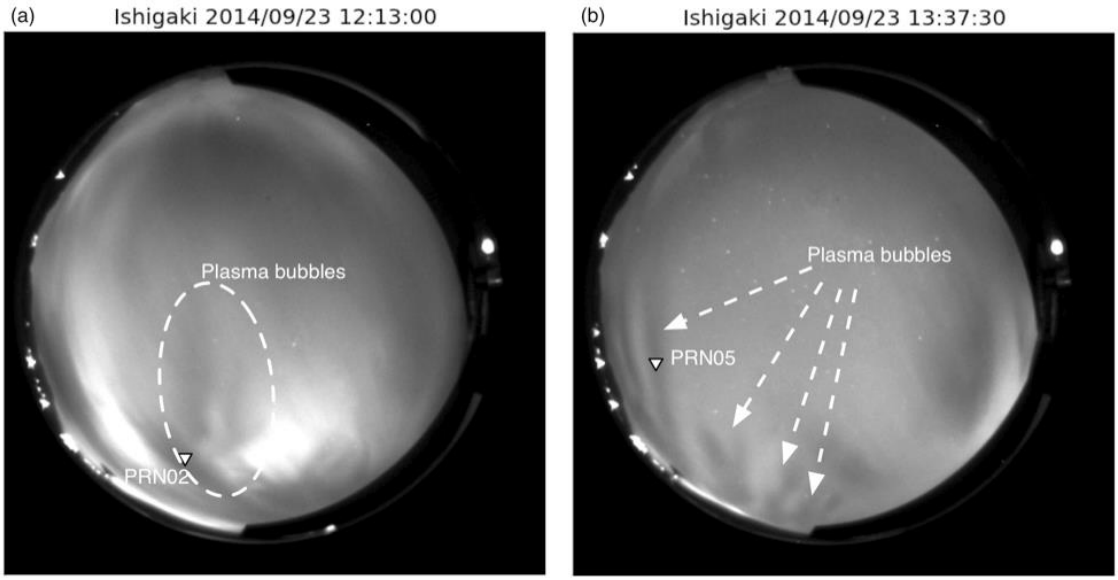

Figure 10. All-sky airglow (630.0 nm) images at (a) 12:23:00 UT and (b) 13:37:30 UT on 23 September 2014 over Ishigaki. Triangles in each figure show the locations of satellites PRN05 and PRN02 at 12:13:00 UT and 13:37:30 UT, respectively.

2.4 GAST-D ground measurements

2.4.1 The GAST-D airborne experimental system was also used to measure the VDB signal power level on the runway surface, which is required by the GAST-D BDS. It was equipped on a vehicle with a VHF V-shaped dipole antenna with an antenna pole of variable length. A GNSS antenna was also equipped to the vehicle. Figure 11 shows the vehicle used for the measurement with an VHF antenna height of 12 ft. Figure 12 shows the raw measured VDB signal strength along the runway center at a height of 12 ft. There were noticeable dips in the measured VDB signal strength.

2.4.2 To investigate the cause of the dips, ray-tracing analysis was conducted with the three-dimensional landscape and buildings taken into account. The deep dips were confirmed to be due to shadowing effects by the control tower located between the runway and the VDB transmitter antenna. The radio propagation analysis with the ray-tracing method is one of the effective ways in locating the VDB transmitter antenna, especially at airports with complex structure.

Figure 11. Measurement vehicle with a VHF antenna at height of 12 ft.

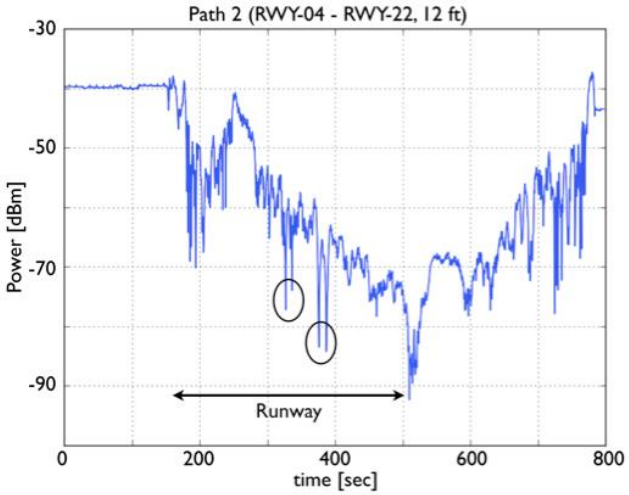

Figure 12. Raw measured VDB signal strength along the runway at a height of 12 ft [7].

2.4.3 Based on the GAST-D airborne experimental system, ENRI is developing a GBAS independent monitor system to record the data and to monitor the user performance of a GBAS. It will be a portable system, and will be a useful tool when a GBAS system is implemented in an airport and its performance is needed to be checked.

3. ACTION BY THE MEETING

3.1 The meeting is invited to:

a) note the information contained in this paper; and

b) discuss any relevant matters as appropriate.

4. REFERENCES

[1] NSP1/-WP26, Summary of GAST-D operational validation program in Japan, Montreal, April 2015.
[2] NSP/1-WP8, GAST-D flight tests at New Ishigaki Airport, Montreal, April 2015.
[3] Yoshihara, T., F. Murashi, S. Saito and K. Hoshinoo, “A Study on Integrity Improvement of GBAS Ground Subsystem Using CSAC (Chip Scale Atomic Clock)”, Proc. of ION ITM 2015, pp.593-599, Dana point, CA, January 2015.
[4] Fujita, S., T. Yoshihara, and S. Saito, Determination of ionospheric gradients in short baselines by using single frequency measurements, J. Aero. Astro. Avi., A- 42, 269–275, 2010.
[5] Saito, S., T. Yoshihara and S. Fujita, “Absolute Gradient Monitoring for GAST-D with a Single-frequency Carrier-phase Based and Code-aided Technique”, Proc. of ION GNSS 2012, pp. 2184-2190, Nashville, September 2012.
[6] Saito, S., T. Yoshihara, and H. Nakahara, Performance of GAST-D ionospheric gradient monitor studied with low latitude ionospheric disturbance data obtained in a real airport environment, ION Pacific PNT 2015, pp. 815-820, Hawaii, April 2015.
[7] NSP/CSG-IP1, Analysis of VDB signal power above runway surface at New Ishigaki Airport, Okinawa, February 2015.

– – – – – – – – – – – – –